AFRL-RX-WP-TP-2011-4235

CREEP AND FATIGUE IN INERT AND VACUUM ENVIRONMENTS OF WOVEN SYLRAMIC-iBN MELT-INFILTRATED COMPOSITES (PREPRINT)

Reji John and Larry Zawada

Metals Branch
Metals, Ceramics, and NDE Division

Gregory N. Morscher

The University of Akron

David Brewer

NASA Langley Research Center

Greg Ojard

Pratt & Whitney

Anthony Calomino

NASA Glenn Research Center

JULY 2011

AIR FORCE RESEARCH LABORATORY
MATERIALS AND MANUFACTURING DIRECTORATE
WRIGHT-PATTERSON AIR FORCE BASE, OH 45433-7750
AIR FORCE MATERIEL COMMAND
UNITED STATES AIR FORCE

REPORT DOCUMENTATION PAGE

Form Approved
OMB No. 0704-0188

1. REPORT DATE *(DD-MM-YY)*	2. REPORT TYPE	3. DATES COVERED *(From - To)*
July 2011	Journal Article Preprint	01 July 2011 – 01 July 2011

4. TITLE AND SUBTITLE
FREQUENCY AND HOLD-TIME EFFECTS ON DURABILITY OF MELT-INFILTRATED SiC/SiC (PREPRINT)

5a. CONTRACT NUMBER
In-house

5b. GRANT NUMBER

5c. PROGRAM ELEMENT NUMBER
62102F

6. AUTHOR(S)
Reji John and Larry Zawada (AFRL/RXLM)
Gregory N. Morscher (The University of Akron)
David Brewer (NASA Langley Research Center)
Greg Ojard (Pratt & Whitney)
Anthony Calomino (NASA Glenn Research Center)

5d. PROJECT NUMBER
4347

5e. TASK NUMBER
20

5f. WORK UNIT NUMBER
LN101100

7. PERFORMING ORGANIZATION NAME(S) AND ADDRESS(ES)

Metals Branch (AFRL/RXLM)
Metals, Ceramics, and NDE Division
Air Force Research Laboratory, Materials and Manufacturing Directorate
Wright-Patterson Air Force Base, OH 45433-7750
Air Force Materiel Command, United States Air Force

The University of Akron
Akron, OH

NASA Langley Research Center
Langley, VA

Pratt & Whitney
East Hartford, CT

NASA Glenn Research Center
Cleveland, OH

8. PERFORMING ORGANIZATION REPORT NUMBER
AFRL-RX-WP-TP-2011-4235

9. SPONSORING/MONITORING AGENCY NAME(S) AND ADDRESS(ES)
Air Force Research Laboratory
Materials and Manufacturing Directorate
Wright-Patterson Air Force Base, OH 45433-7750
Air Force Materiel Command
United States Air Force

10. SPONSORING/MONITORING AGENCY ACRONYM(S)
AFRL/RXLM

11. SPONSORING/MONITORING AGENCY REPORT NUMBER(S)
AFRL-RX-WP-TP-2011-4235

12. DISTRIBUTION/AVAILABILITY STATEMENT
Approved for public release; distribution unlimited.

13. SUPPLEMENTARY NOTES
PAO Case Number: 88ABW 2010-2171; Clearance Date: 21 Apr 2010. Document contains color.
Journal article submitted to *Composites Science & Technology*.

14. ABSTRACT
In order to better understand the effect of stressed-oxidation, the performance of woven Sylramic-iBN fiber-reinforced slurry cast melt-infiltrated (MI) composites were tested in creep and fatigue under non-oxidizing conditions. Initially creep and fatigue tests were performed at 1204 °C in an argon atmosphere; however, it was observed that sufficient oxidizing species existed in the environment to degrade the composites in a manner similar to air environments. Therefore, creep and fatigue tests were performed at 1204 °C in a vacuum environment which showed no evidence of oxidation and superior properties to composites subjected to stressed-oxidation conditions. The mechanical results and microscopy of the vacuum and argon are compared to the behavior of these composites tested in air. It was found that the stress rupture properties of the vacuum-tested composites could be predicted from single fiber creep rupture data assuming reasonable values for the Weibull modulus.

15. SUBJECT TERMS
stressed-oxidation, Sylramic-iBN, melt-infiltrated (MI) composites

16. SECURITY CLASSIFICATION OF:			17. LIMITATION OF ABSTRACT:	18. NUMBER OF PAGES	19a. NAME OF RESPONSIBLE PERSON (Monitor)
a. REPORT	b. ABSTRACT	c. THIS PAGE			Reji John
Unclassified	Unclassified	Unclassified	SAR	34	19b. TELEPHONE NUMBER *(Include Area Code)* N/A

To be submitted, Composites Science and Technology, 2010.

Creep and Fatigue in Inert and Vacuum Environments of Woven Sylramic-iBN Melt-Infiltrated Composites

Gregory N. Morscher[2], Reji John[1], Larry Zawada[1], David Brewer[3], Greg Ojard[4], and Anthony Calomino[5]

[1] Air Force Research Laboratory, AFRL/RXL, Wright-Patterson AFB, OH
[2] The University of Akron, Department of Mechanical Engineering; Akron OH
[3] NASA Langley Research Center, Langley VA
[4] Pratt & Whitney, East Hartford, CT
[5] NASA Glenn Research Center, Cleveland, OH

ABSTRACT

In order to better understand the effect of stressed-oxidation, the performance of woven Sylramic-iBN fiber-reinforced slurry cast melt-infiltrated (MI) composites were tested in creep and fatigue under non-oxidizing conditions. Initially creep and fatigue tests were performed at 1204^{o}C in an argon atmosphere; however, it was observed that sufficient oxidizing species existed in the environment to degrade the composites in a manner similar to air environments. Therefore, creep and fatigue tests were performed at 1204^{o}C in a vacuum environment which showed no evidence of oxidation and superior properties to composites subjected to stressed-oxidation conditions. The mechanical results and microscopy of the vacuum and argon are compared to the behavior of these composites tested in air. It was found that the stress rupture properties of the vacuum-tested composites could be predicted from single fiber creep rupture data assuming reasonable values for the Weibull modulus.

INTRODUCTION

A composite system of interest for hot-section gas turbine applications is the woven Sylramic-iBN fiber-reinforced slurry cast melt-infiltrated (MI) composite system [1]. In order to understand the creep and fatigue properties as well as damage accumulation of this system in oxidizing environments, several studies have been performed which cover a wide range of stress, time, and fatigue conditions at 1200^{o}C [2-3]. However, to better understand the effect of environment on creep rupture or fatigue at

elevated temperatures, it is necessary to determine the creep rupture and fatigue properties in an inert environment.

The deleterious effect of oxidative environments on SiC fiber reinforced composites due to the oxidation of the fiber, interphase, and matrix through surface exposed matrix cracks has been well documented, especially at temperatures below which creep effects become dominant [4-9]. There have been a few studies where creep or fatigue of SiC/SiC composites were performed in air and inert environments at temperatures $\geq$ 1200^{o}C. For example, Zhu et al. [8] performed creep and/or fatigue experiments at 1300^{o}C with Nicalon^{TM} and Hi-Nicalon^{TM} reinforced woven CVI matrix composites in air and argon environments. It was observed that Nicalon^{TM} CVI matrix composites exhibited superior time-to-failure performance in argon environments. However, somewhat surprisingly, Hi-Nicalon reinforced CVI SiC composites had better creep performance in air than in argon [8]. Chermant and coworkers [9-11] have performed several studies where creep was performed in air and argon environments on Nicalon^{TM} and Hi-Nicalon^{TM} reinforced CVI SiBC matrix composites. Though the emphasis of these papers were on damage mechanisms controlling creep behavior, it was evident for the Hi-Nicalon^{TM} CVI SiBC system that creep rupture times in argon at 1200^{o}C and 1300^{o}C were longer than for composites tested in air. For example, the run out condition of 200 hours occurred 20 MPa higher for argon tested (170 MPa) than for air tested (150 MPa) for creep at 1200^{o}C. Martinez-Fernandez and Morscher also demonstrated superior stress-rupture performance from 750 to 1200^{o}C for single tow Hi-Nicalon^{TM} CVI SiC matrix minicomposites with C and BN interphases tested in vacuum [12] compared to similar minicomposites tested in air [13].

The goal of this work was to determine the effect of environment on the 1200^{o}C creep and fatigue performance of the woven Sylramic-iBN MI SiC matrix composite system by performing similar tests to reference 3 in inert environments in order to understand or at least approach the “intrinsic” creep-rupture properties of this composite system. From this, a true assessment of the effect of environment, e.g., tests performed in reference 3, can be ascertained.

EPERIMENTAL

Creep rupture and 1 Hz fatigue (R = 0.1) were performed on woven 7.9 tow ends per cm (epcm) five-harness Sylramic-iBN fiber-reinforced melt-infiltrated (MI) composites with a BN interphase at 1204^{o}C. Each fiber tow consists of 800 filaments with an average diameter of 10 microns each. The Sylramic^{TM} as-produced fiber was produced by Dow Corning, Midland MI, but is now available for ATK COI Ceramics in San Diego CA. The woven fiber plies were subject to a further NASA-proprietary treatment in order to improve the creep-resistance of the fiber and to create an in-situ BN layer on the surface of the each individual fiber. This composite system is commonly referred to as N24A developed by NASA under the UEET program [14] and consists of an eight ply lay-up with each ply aligned in the 0/90 direction. Tensile test specimens were on the order of 155 mm length and grip width of ~ 12 mm with a tapered dogbone section with ~ 8.2 mm width straight edges over a 40 mm gage section.

The creep rupture tests were performed with an Instron universal testing machine fitted with an environmental chamber at NASA Glenn Research Center. A graphite element furnace was used to heat the specimens in the gage section. Contact extensometers employing SiC contact rods and an LVDT were used to measure strain. The environment was either gettered Argon (99.999%) or vacuum (10-5 Torr). Specimens that survived the run-out condition (500 hours) were removed from the test and tested at room temperature in the same manner (unload-reload to failure) as reference 3 in order to determine residual properties.

After the creep rupture or residual tensile test to failure, one section of the fracture surface was cut and polished (~ 1mm from the edge) in the longitudinal direction in order to determine the nature of matrix cracking in the composite. The other portion of the fracture surface was observed in the field emission scanning electron microscope (FESEM, model Hitachi 4700, Tokyo Japan).

RESULTS

The rupture and fatigue data are shown as stress versus time (Figure 1) and strain versus time (Figure 2). ***Initially, creep tests were performed in an Argon*** environment; however, after two tests it became obvious that failure times were similar to that of air-tested composites (Figure 1 and 2). FESEM was performed for the two specimens and it

was obvious that oxidation was occurring in the matrix crack which caused strong fiber-to-fiber a fiber-to-matrix bonding as a result of fiber, interphase, and matrix oxidation. Figure 3 shows a stereo-optical micrograph of the fracture surface and FESEM images of one of the corners of the fracture surface. Oxidation of fiber surfaces and a relatively flat fracture surface is evident at and around the corner of the specimen. This was apparent at all four corners of the specimen and most of the face near the surface of the specimen on the one side of the specimen. The interior of the fracture surface was relatively pristine with BN clearly present at the interphase and fiber pullout prevalent. It is obvious that stressed-oxidation induced premature fiber failure and unbridged crack growth prior to ultimate failure led to the shorter than expected lifetimes. This behavior is very similar to that observed in air tests [3]. This was surprising. The oxygen concentration based on the effluent from the chamber prior to sealing the gettered chamber was less than 20 ppm oxygen. It was decided that in order to assess the creep and fatigue effect for a non-oxidizing environment, this Argon environment was abandoned in favor of a vacuum environment. However, this does show that even in very low oxygen containing environments and at these higher stresses, these composites degrade to the same degree as oxygen contents ~ 10,000 times greater (i.e., air). It should be noted thought, that an earlier study with effluent measurements on the order of 5 to 10 ppm oxygen content for creep of SiC fiber-reinforced calcium alumino silicate matrix composite did not report evidence of oxidation embrittlement [15].

Creep in vacuum proved to be much more long lasting (Figure 1). Initially two creep tests and one fatigue test were performed at the 220 MPa stress level with all specimens exceeding the run-out condition of 500 hours with no failures. The lifetimes for four air and argon tested specimens subjected to 220 MPa ranged from 17 to 154 hours [3]. Therefore, the stress was increased to 248 MPa for the next vacuum creep tests, both of which ruptured prior to the run-out condition (188 and 469 hours for the two specimens). This was still superior to air creep at 248 MPa by over an order of magnitude in time (0.5 and 3.5 hours for two air-tested specimens [3]). Finally, a 262 MPa creep test in vacuum was performed with ruptured after 161 hours.

Not only were the creep rupture times for vacuum tested specimens longer than air-tested specimens or the argon-tested of this study, the strain and strain-rates were

lower for the vacuum-tested compared to the other two conditions for the same 220 MPa applied stress condition (Figure 2). It does not appear that a true steady-state strain rate has been reached. However, the effective strain rates for the air and vacuum test data (Figure 2) differ by two orders of magnitude. The total strain of the air-tested specimen that survived the longest time (~ 150 hours and ~ 0.3% total strain) reached nearly twice the total strain compared to the vacuum tested specimen (~ 0.18 % total strain). It is evident that the oxidation processes are contributing to not only shorter lives but also higher strain and strain rates under the same conditions.

The three specimens that survived the 220 MPa creep and fatigue run-out conditions in vacuum were tensile (load-unload-reload) tested to failure at room temperature (Figure 4). Excellent retained properties were measured for the three specimens (381 + 27 MPa), approximately 81% of the as-produced tensile strength of the composite. Note that the residual stress in the matrix was observed to increase for these specimens due to creep of the matrix (similar to reference 3). However, it appears that the fatigue condition showed less of an increase in residual stress compared to the constant stress creep condition.

Figure 4 shows two typical vacuum-tested fracture surfaces, one of a specimen which survived the 220 MPa 500 hour creep rupture condition followed by room temperature residual tensile-to-failure test (Figure 5a) the other of a specimen which ruptured at 248 MPa in vacuum after 469 hours (Figure 5b). No evidence of oxidation was evident in any of the fracture surfaces for specimens tested in vacuum. BN was always present and debonding and pull out was observed either between the fiber/BN interface or between the BN/matrix interface.

One half of the tensile bar gage section was cut and polished longitudinally along the edge of the specimen in order to observe the character of matrix cracking. Figure 6 shows an example of a vacuum tested specimen subjected to 248 MPa creep stress that ruptured after 469 hours. Note that matrix cracks are evident. However, there are no large scale unbridged regions of matrix cracks typical of the air [3] and inert tested specimens at this stress (Figure 7). By large scale, it is meant that all the fibers in a tow(s) perpendicular to a matrix crack in the crack wake had failed at some point prior to final ultimate failure (the same observation is made in the fracture surface (Figure 3)). All of

the vacuum tested specimens have been examined and not one instance of an unbridged crack like that in Figure 7 can be found. It should be noted that the melt-infiltrated portion at the surface of the specimen of the matrix was depleted of Si during the vacuum test presumably due to Si vaporization (Figure 6). The CVI SiC and the fibers themselves appeared not to be affected at this temperature.

It is interesting to note that the actual stress-dependent density of cracks along the length is essentially the same for the air tested [3] and the vacuum tested specimens (Figure 8). This implies that the "extra strain" accumulated during air tests are not associated with an increase in crack density. However, some air-tested cracks have unbridged regions as already discussed which would increase the strain per crack. In addition, oxidation of the interface could lead to possible decoupling near the crack surface followed by re-bonding after glass formation. It would be expected that matrix crack depth would increase for air-tested composites for lower stress conditions; however, it is interesting that even for the 220 MPa stress in air, few if any cracks were through-the-cross section. However, it was evident that cracks in air-tested specimens could grow two or three plies deep in effectively the same "plane" perpendicular to the stress direction. Whereas for the vacuum tested specimens, the cracks do not appear to align in the same "plane" and may or may not be linked up to one another, even for the 248 MPa creep condition (Figure 6).

MODELING COMPOSITE RUPTURE

Though the vacuum creep and fatigue was superior to air-tested creep and fatigue, there still was stress/time dependent degradation for the vacuum tested composites. If the vacuum creep rupture data is related to fiber creep-rupture properties without the influence of fiber-fiber strong bonding due to oxidation, one should be able to relate the creep rupture behavior of the fibers to the creep rupture data of the vacuum tested composites from global load sharing considerations. There is some creep rupture fiber data for the Syl-iBN fibers available in the literature [16]. The data in reference 16 was plotted as a Larson-Miller for tests ranging from 900 to 1400^{o}C and converted here to a stress vs. time plot at 1204^{o}C for 25mm gage length single fiber creep rupture data as shown in Figure 9. For 1204^{o}C, the fiber stress rupture can be described by:

$$\sigma_{fiber}\,(t, 1204^{o}C) = 1010.7\ t^{-1/11.1} \qquad (1)$$

The model of Halverson and Curtin [17] was employed in this study. Their model relates the time-dependent strength properties of individual fibers to time-dependent composite properties. The model is somewhat complex and iterative, but in general the iterative steps of the model are as follows:

1. For an applied stress at a given temperature and increment of time, the amount of fiber-breakage at and around a through-thickness crack is determined base on individual time-dependent fiber failure properties and Weibul statistics (e.g., Figure 9) taking into consideration the stress-transfer to the fibers from the matrix due to the interfacial shear stress, τ, between the fibers and the matrix (Figure 10).
2. Then the new stress state of the remaining unbroken fibers in the matrix crack is determined and the next increment of time is employed to determine the amount of new fiber-breakage and the new and increased stress state on the remaining fibers
3. The iteration is continued until the remaining fibers can no longer carry the increased loads from the broken fibers, i.e., the time for composite rupture under that constant applied composite stress condition.

Different matrix crack spacing conditions were modeled by Halverson and Curtin [17], which ranged from the case where (1) there is a single matrix crack or the matrix crack spacing is so large that a given matrix crack is not influenced by neighboring cracks and (2) matrix crack spacing is small if not saturated and the sliding lengths of neighboring matrix cracks would interact (i.e., matrix cracks are closer to one another than the fiber sliding length as determined from the interfacial sliding stress, τ). For the case of this study, the former case can be employed since matrix crack spacing is quite large, i.e., the matrix crack density is quite small compared to the saturation crack density of this composite which is about 9 cracks/mm (see Figure 6).

The details of the model will not be repeated here but can be found in [17]. The key relationship to be solved is equation 30 from reference 17:

$$\frac{\sigma}{f_o} = \left[1 - q\left(1 + \frac{T\delta_c}{2\sigma_c x}\right)\right]T \tag{2}$$

Where q is the probability of failure of a fiber (equation 24 in reference 17 – see Appendix A) which is dependent on the time-dependent properties of the fibers, sliding length, number of cracks, T is the average peak stress on the remaining fibers in the matrix crack (Figure 10), x is the crack spacing, and the characteristic stress, σ_c, and characteristic sliding length, δ_c, are as follows [18]:

$$\sigma_c = \left(\frac{\sigma_o^m l_o \tau}{r}\right)^{\frac{1}{m+1}} \tag{3}$$

$$\delta_c = \frac{r\sigma_c}{\tau} \tag{4}$$

where σ_o is the fiber strength at a given gage length l_o, m is the Weibull modulus of the fiber strength distribution, and r is the fiber radius. σ_c of the as-processed fibers at 1204^{o}C in the composite can also be derived from the ultimate tensile strength of the composite, σ_{UTS}, tested at 1204^{o}C from the relationship [19]:

$$\sigma_c = \frac{\sigma_{UTS}}{f_o}\left(\frac{m+1}{m+2}\right)\left(\frac{2(m+1)}{m(m+2)}\right)^{-1/(m+1)} \tag{5}$$

Then, the in-situ strength of individual fibers after composite fabrication at 1204^{o}C, σ_o, can be estimated by using σ_c from equation 5 and solving for σ_o in equation 3 for a 25 mm gage length (l_o) which is necessary for the determination of the slow crack growth parameters described in Appendix A (equation A6) as they relate to the 25 mm gage length fiber stress rupture data of Figure 9.

Equation 2 is used to determine the new stress state in the fibers after an increment of time at an applied stress. One solves equation 2 for T (the new stress on the remaining fibers after a number of fibers failed due to q) iteratively over an increment of time that is relatively small compared to the failure time. After each iteration, a new q is determined based on the new T. This process is continued until there no longer is a solution for equation 2 (which is the case where there are no longer any fibers remaining

to carry the applied stress). The determination of q and appropriate time-dependent fiber properties are discussed in Appendix A. The time increment used for the iterations was 1 hour. τ was determined in the same manner as reference 20 where the non-linearity in the fast fracture stress strain curves performed on the same composite material at 1204^{o}C was modeled by best-fitting the extra displacement of each crack due to τ assuming the stress-dependent matrix crack density of Figure 8. A τ value of ~ 40 MPa was determined for 1204^{o}C, which is lower than the ~ 70 MPa typical determined for this composite at room temperature [20]. The fiber Weibull modulus for Sylramic fibers has been reported to be ~ 5 [21] at room temperature. A more recent study found the fiber Weibull modulus to be ~ 2.5 for Sylramic-iBN [22] at room temperature. It is not known what the Weibull modulus is for high temperature fiber fast fraction, so values ranging from 3 to 5 were used based on room temperature data (the data for m = 4 and 5 are shown in Figure 11 since it envelopes the data).

Table I shows the parameters used to model stress rupture behavior and Figure 11 shows the model results compared to the vacuum tested stress rupture behavior. The model predicts the composite rupture data quite well for m between 4 and 5. Accurate measures of m and σ_o at 1204^{o}C would be useful to further refine the model; nevertheless, this result is considered excellent and is only based on measured or very reasonable estimates of constituent or composite properties.

The individual fiber data from Figure 9 is also plotted in Figure 11 multiplied by the fiber volume fraction in the loading direction. The 25 mm single fiber data rupture behavior normalized by fiber fraction is much lower than the vacuum tested composite. This would be expected due to different local fiber loading length scales within matrix cracks and global load sharing conditions for the composite. However, it is interesting that the long-time air-tested composite stress rupture data is similar to 25 mm single fiber data adjusted for fiber volume fraction. This may not be serendipitous, rather it probably relates to failure of single or multiple tows in a fiber-bridged matrix microcrack (cracks are not through-the-thickness at stresses below 220 MPa). In a microcrack that extends from the surface of the composite, fibers bridging the microcrack will be fused together due to the result of BN and SiC oxidation and a single fiber failure event, due to strong bonding between local fibers, can result in mass fiber failure of all the strongly bonded

fibers within that microcrack. This is similar to the low stress, long time intermediate temperature condition modeled in Reference 23.

DISCUSSION

The nearly intrinsic time-dependent composite rupture properties determined for the woven Sylramic-iBN fiber-reinforced melt-infiltrated SiC matrix composite tested in this study at 1204^{o}C were superior to the rupture properties of the same material in tested under similar conditions in air [3]. Since fibers failed in a global manner, the stress rupture behavior of the composite could be modeled from individual fiber data and measured fiber properties with good agreement based on the model of Halverson and Curtin [17].

The difference in stress rupture properties between vacuum and air environments (for a 500 hour life a difference in stress-carrying ability of over 75 MPa between vacuum and air – see Figure 1) is indicative of the stressed-oxidation mechanisms in air for this composite system. The agreement of the Halverson Curtin model with the rupture data based on fiber rupture properties establishes the fiber properties appropriate to model the air-tested specimens. However, further mechanisms of stressed-oxidation failure will have to be incorporated in future modeling efforts similar to [23] including the kinetics for oxygen ingress and fiber-to-fiber strong bonding as well as the mechanics for non-through-thickness matrix cracks [3] most likely due to stress relaxation in the matrix at these temperatures.

Another interesting result of this study was that specimens tested in high purity Argon with oxygen concentrations no greater than 20 ppm resulted in oxidation of the BN interphase and subsequent bonding of fibers to one another similar to that observed in air. This was very surprising and is another area that requires greater investigation. Nonetheless, the fact that the rupture properties in the 20 ppm O_2 Argon environment were about the same as that in air indicates that the concentration of oxygen, at least from 20 ppm to 200,000 ppm, does not have a strong effect on stressed-oxidation degradation, but rather the presence of oxygen (at least above 20 ppm) is most significant. Even so, the stress-rupture properties of this composite system at 1204^{o}C in air are still superior to other composite systems tested in air with similar fiber volume fractions.

CONCLUSIONS

Creep and fatigue of a state-of-the-art woven Sylramic-iBN fiber-reinforced melt-infiltrated SiC matrix composite system was determined in inert environments at 1204^{o}C. It was demonstrated for the condition where no oxidation effects were present, i.e., vacuum, creep and fatigue properties were far superior to that of air-tested composites at 1204^{o}C. The argon atmosphere proved to contain enough oxygen (< 20 ppm) to result in embrittlement effects and stressed-oxidation properties similar to air. Stress-dependent matrix crack densities for vacuum tested specimens were similar to air-tested data; however, the vacuum tested specimens did not show any unbridged matrix crack growth, with the exception of the final failure crack, unlike the air or argon tested specimens where unbridged (fiber-failure in the crack wake) regions of matrix cracks away from the fracture surface were common. It was shown that the vacuum-tested data appeared to behave in a manner expected from that measured for individual fiber creep rupture experiments based on the model of Halverson and Curtin. This understanding will next be employed to develop time-dependent stressed-oxidation models for the oxidizing environments.

APPENDIX A: DETERMINATION OF "q"

In reference 17, q is defined as the "probability of failure of a fiber, with respect to time" that corresponds to the stress profile shown in Figure A1:

$$q\left(\tilde{T},l_s,\tilde{t}\right)=1-\exp\left\{-\tilde{T}\times\left[\int_{\alpha}^{1}\left(x^{\beta-2}\tilde{T}^{\beta-2}+\int_{0}^{\tilde{t}}x^{\beta}\tilde{T}(t')^{\beta}dt'\right)^{m/(\beta-2)}dx+\alpha^{m+1}\left(\tilde{T}^{\beta-2}+\int_{0}^{\tilde{t}}\alpha T(t')^{\beta}dt'\right)^{m/(\beta-2)}\right]\right\} \quad \text{(A1)}$$

The dimensionless parameters $\tilde{T}$, α, and $\tilde{t}$ are defined as:

$$\tilde{T}=\frac{T}{\sigma_c} \quad \text{(A2)}$$

$$\alpha=\frac{\sigma_{ff}}{\sigma(z=0)}=f\left(\frac{E_f}{E_c}\right) \quad \text{(A3)}$$

$$\tilde{t} = tC\sigma_c^2 \tag{A4}$$

where σ_{ff} is the far field stress ($z \geq \delta$) and t is time. The parameters β and C are the slow crack growth parameters from equation 20a in reference 17:

$$\sigma(t) = \left(\sigma_o^{\beta-2} + C\int_0^{\tilde{t}} \tilde{T}(t')^{\beta}\, dt' \right) \tag{A5}$$

where $\sigma(t)$ is the fiber strength after some time at stress T due to the growth of a pre-existing flaw and σ_o is the initial fiber strength corresponding to that initial flaw size. When one assumes that T is constant over the integration time and σ_o, the stress corresponding to the initial flaw size at t = 0, is much larger than $\sigma(t)$. Then:

$$Ct = \sigma_o^{\beta-2} / \sigma^{\beta} \tag{A6}$$

and the parameters C and β can be best fit to describe the time-dependent strength data of the fibers (Figure 9).

ACKNOWLEDGEMENTS

We would like to thank John Zima of the University of Toledo for running the vacuum tests, Professor William Curtin for discussions concerning the use of his model, and Thomas Smith for programming assistance. This effort was partially funded by Air Force Research Laboratory, Materials and Manufacturing Directorate under a subcontract through University of Dayton Research Institute. All tests were performed at NASA Glenn Research Center.

REFERENCES

1. J.A. DiCarlo, H-M. Yun, G.N. Morscher, and R.T. Bhatt, "SiC/SiC Composites for 1200°C and Above" ***Handbook of Ceramics Composites,*** Chapter 4; pp. 77-98 (Kluwer Academic; NY, NY: 2005).
2. Kalluri S, Calomino AM, Brewer DN. Comparison of elevated temperature tensile properties and fatigue behavior of two variants of a woven SiC/SiC composite. Ceram Eng Sci Proc 2005;26(2):303–10.

3. G.N. Morscher, G. Ojard, R. Miller, Y. Gowayed, U. Santhosh, J. Ahmed, and R. John, “Tensile Creep and Fatigue of Sylramic-iBN Melt-Infiltrated SiC Matrix Composites: Retained Properties, Damage Development, and Failure Mechanisms” *Comp. Sci. Tech.*, 68 3305-3313 (2008)
4. Heredia, F. E., McNulty, J. C., Zok, F. W. and Evans, A. G., Oxidation embrittlement probe for ceramic-matrix composites. J. Am. Ceram. Soc., 1995, 78, 2097.
5. Lin, H. T. and Becher, P. F., Effect of coating on lifetime of Nicalon fiber-silicon carbide composites in air. Materials Science andEngineering , 1997, A231, 143–150.
6. Morscher, G. N., Tensile stress-rupture of SiCf/SiCm minicomposites with carbon and boron nitride interphases at elevated temperatures in air. J. Am. Ceram. Soc., 1997, 80, 2029–2042.
7. Morscher, G. N., Hurst, J. and Brewer, D., Intermediate-temperature stress rupture of a woven Hi-Nicalon, BN-interphase, SiC-matrix composite in air. J. Am. Ceram. Soc., 2000, 83, 1441–1449.
8. S.Zhu, M. Mizuno, Y. Kagawa, J.Cao, Y.Nagano, and H. Kaya, "Creep and Fatigue Behavior in Hi-NicalonTM - Fiber-Reinforced Silicon Carbide Composites at High Temperature," J.Am.Ceram.Soc., 82[1]117-28(1999)
9. J.L. Chermant, G. Boitier, S. Darzens, G. Farizy, J. Vicens, J.C. Sangleboeuf, "The creep mechanism of ceramic matrix composites at low temperature and stress, by a material science approach," J. Eur. Ceram. Soc., 22 2443-2460 (2002)
10. S.Darzens, J-L Chermant, and J-C. Sangleboeuf, "Advantages of SiC Hi-Nicalon or NLM 202 Fibers in SiCf-SiBC Composites," J.Am.Ceram.Soc., 88[7]1967-1972(2005)
11. G.Farizy, J-L. Chermant, J. Vicens, and J-C. Sangleboeuf, "Understanding of the Behavior and the Influence of Oxidation During Creep of SiCf-SiBC Composites in Air," Adv. Eng. Materials., 7 [6] 529-535 (2005)
12. J. Martínez Fernández and G. N. Morscher, “Tensile Stress-Rupture of SiC/SiC Minicomposites in Vacuum,” *Ceram. Eng. Sci. Proc*, **22** [3] 561-568 (2001)

13. J. Martinez-Fernandez and G.N. Morscher, “Room and Elevated Temperature Tensile Properties of Single Tow Hi-Nicalon, Carbon Interphase, CVI SiC Matrix Minicomopsites,” J. Euro. Ceram. Soc., 2000, 20 [14-15], 2627-2636.
14. J.A. DiCarlo, H-M. Yun, G.N. Morscher, and R.T. Bhatt, "SiC/SiC Composites for 1200^{o}C and Above" Handbook of Ceramics Composites, Chapter 4; pp. 77-98 (Kluwer Academic; NY, NY: 2005)
15. X. Wu and J. Holmes, “Tensile Creep and Creep-Strain Recovery Behavior of Silicon Carbide Fiber/Calcium Aluminosilicate Matrix Ceramic Composites,” *J. Am. Ceram. Soc.,* **76** [10] 2695-700 (1993).
16. H.M. Yun, D. Wheeler, Y. Chen, and J.A. DiCarlo, “Thermo-Mechanical Properties of Super Sylramic SiC Fibers,” Ceram. Eng. Sci. Proc., 2005
17. H.G. Halverson and W.A. Curtin, “Stress Rupture in Ceramic-Matrix Composites: Theory and Experiment,” *J. Am. Ceram. Soc.,* **85** [6] 1350-65 (2002)
18. W.A. Curtin, “Theory of Mechanical Properties of Ceramic-Matrix Composites,” J. Am. Ceram. Soc., 74 [11] 2837-45 (1991)
19. W.A. Curtin, B.K. Ahn and N. Takeda, “Modeling brittle and tough stress-strain behavior in unidirectional ceramic matrix composites”, *Acta mater.* **46** 3409-3420 (1998).
20. G.N. Morscher, “Stress-Dependent Matrix Cracking in 2D Woven SiC-fiber Reinforced Melt-Infiltrated SiC Matrix Composites”, *Comp. Sci. Tech.*, 64 pp. 1311-1319 (2004)
21. J. Hurst, H.-M. Yun, and D. Gorican, ‘‘A Comparison of the Mechanical Properties of Three Polymer-Derived Small Diameter SiC Fibers; pp. 3–15 in Ceramic Transactions, Vol. 74, *Advances in Ceramic-Matrix Composites III.* Edited by N. P. Bansal and J. P. Singh. American Ceramic Society, Westerville, OH, 1996.
22. C. Smith, “Monitoring Damage Accumulation in SiC/SiC Ceramic Matrix Ccomposites Using Electrical Resistance,” Masters Thesis, University of Akron (2009)

23. G.N. Morscher and J.D. Cawley, "Intermediate Temperature Strength Degradation in SiC/SiC Composites," *J. European Ceramic Society*, vol. 22, no. 14-15, pp. 2777-2788 (2002)
24. Marshall, D.B., Cox, B.N., and Evans, A.G., "The mechanics of matrix cracking in brittle-matrix fiber composites" *Acta metal.*, **33**, 2013-2021 (1985).

Table I: Parameters used in Model

f_o	0.19
σ_{UTS} (1200°C)	415 MPa
E_f	380 GPa
E_m	235 GPa
τ	40 MPa
m	3 to 5
β	11.1
C*	9.0 E-6 (for m = 5) 1.0 E-6 (for m = 4) 1.0 E-7 (for m = 3)

* C depends on the σ_o value used to best fit the fiber rupture data (Equation A6) which is dependent on m.

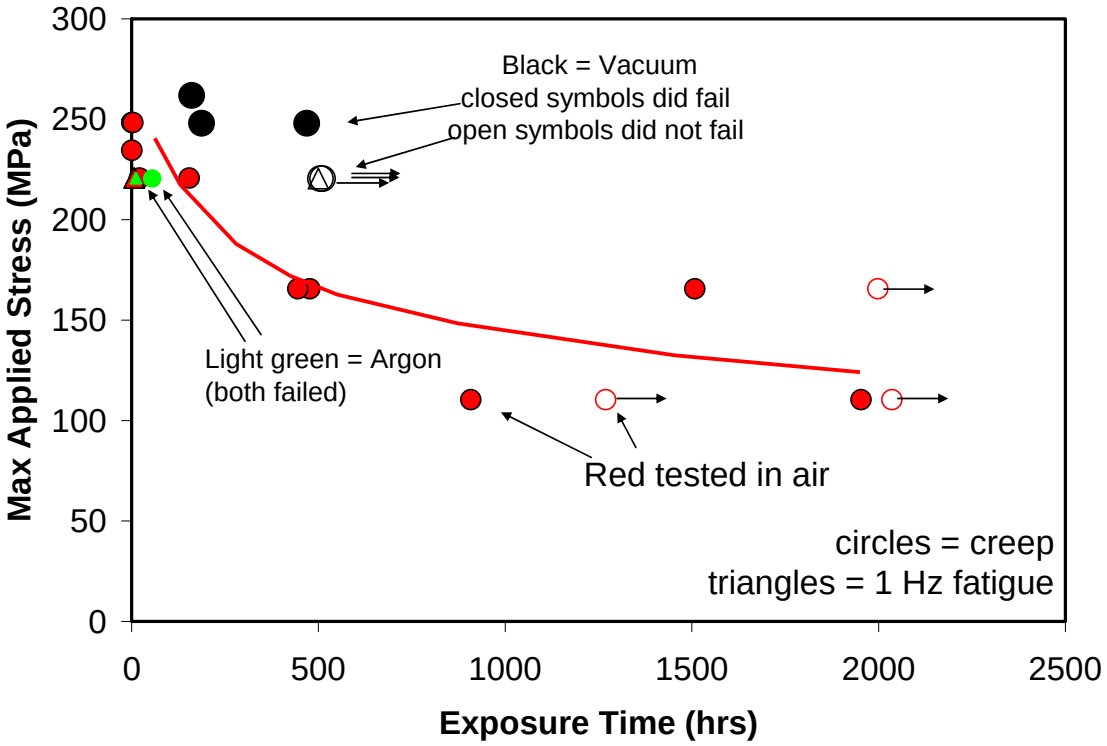

Figure 1: Creep rupture and fatigue of inert and air [3] experiments.

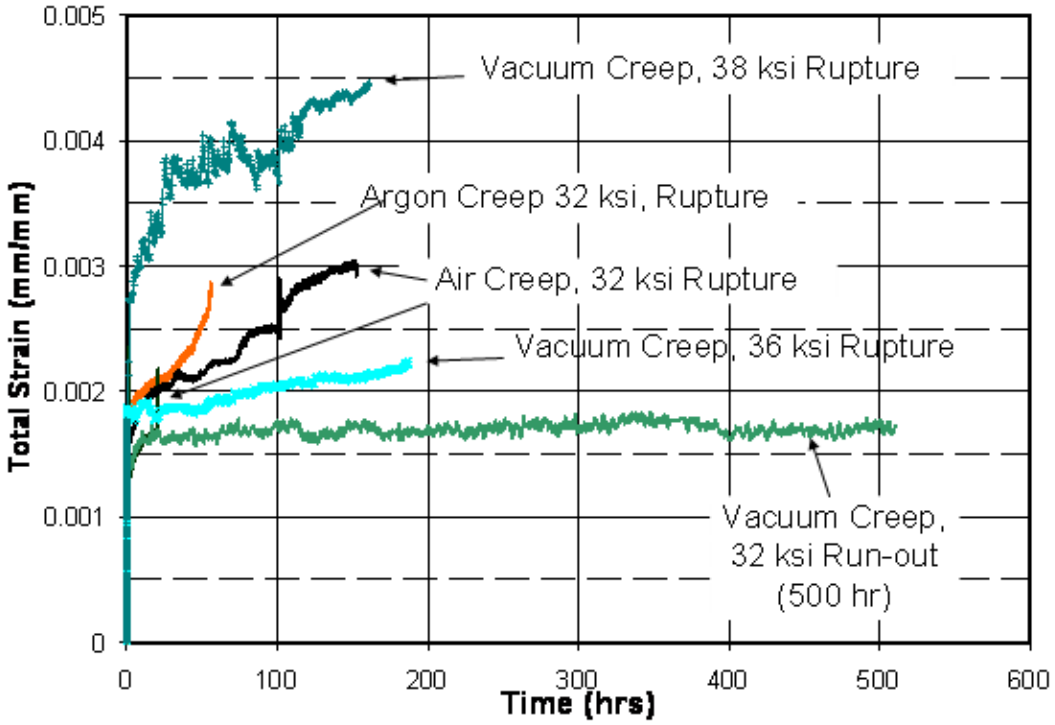

Figure 2: Total strain accumulation during creep tests.

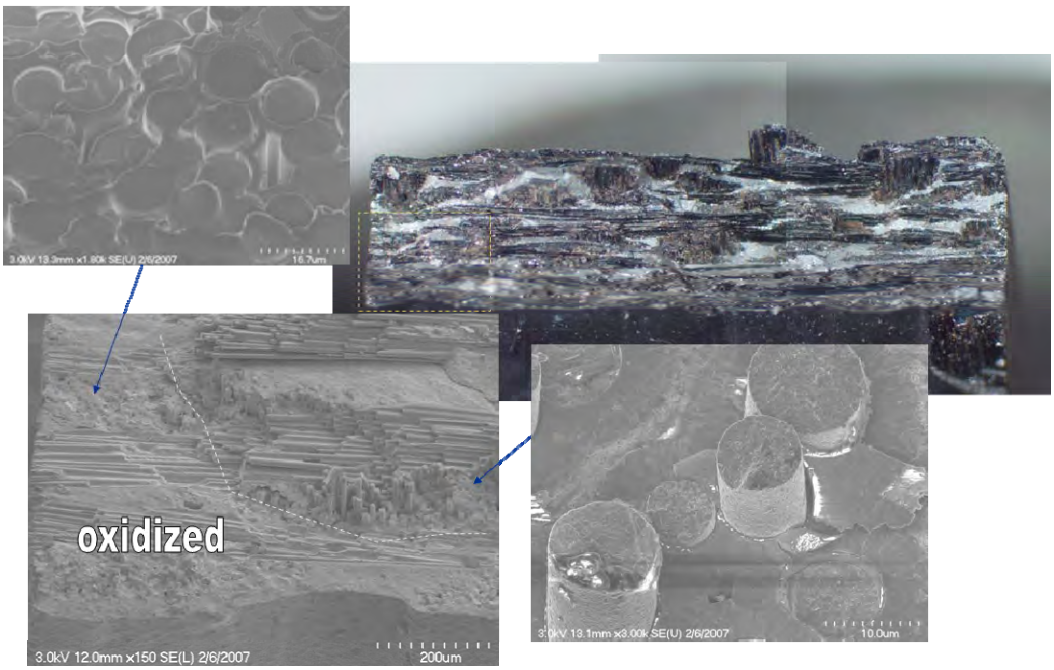

Figure 3: Fracture surface from 220 MPa Argon creep-rupture specimen.

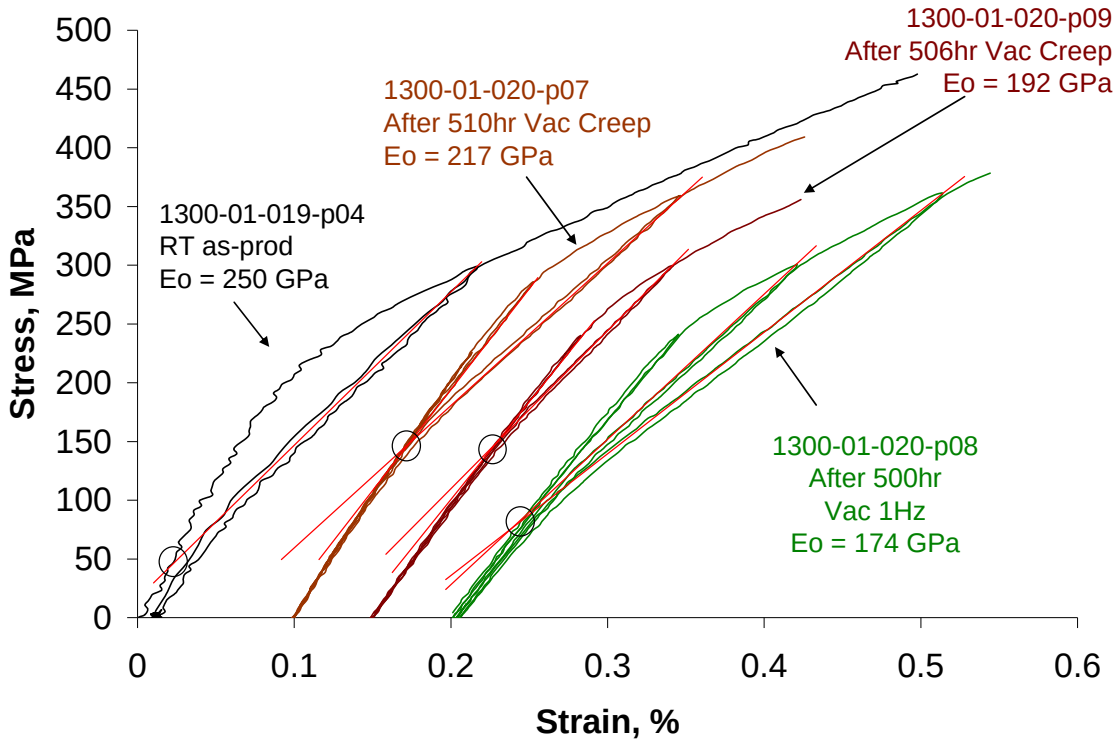

Figure 4: Room temperature retained tensile curves for the three vacuum tested specimens compared to a typical as-produced specimen [3].

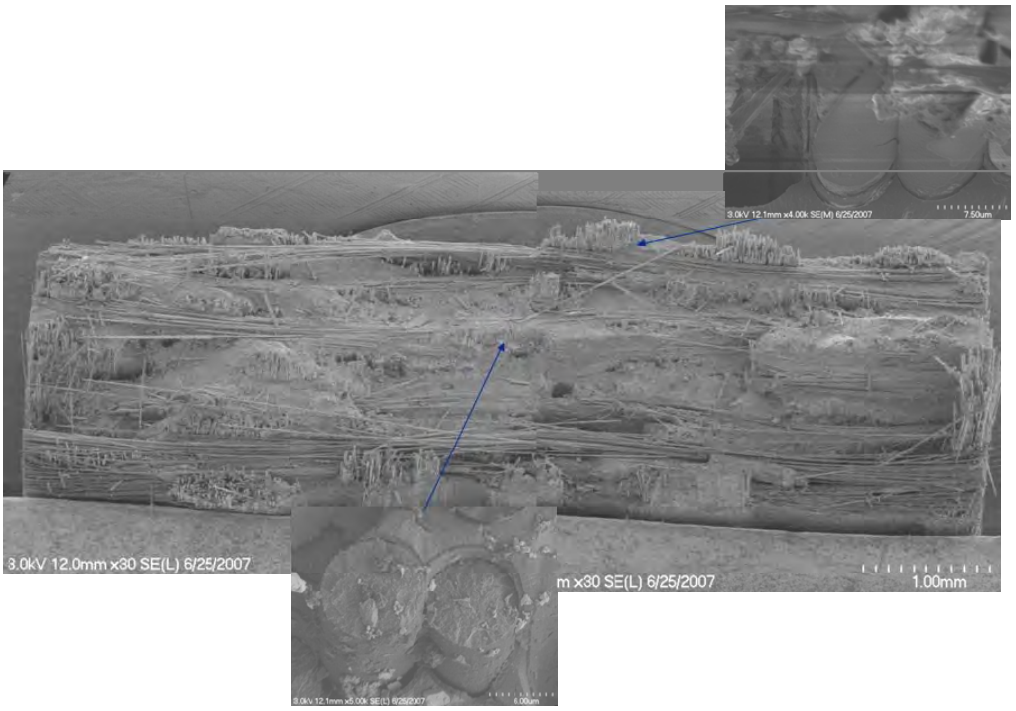

(a)

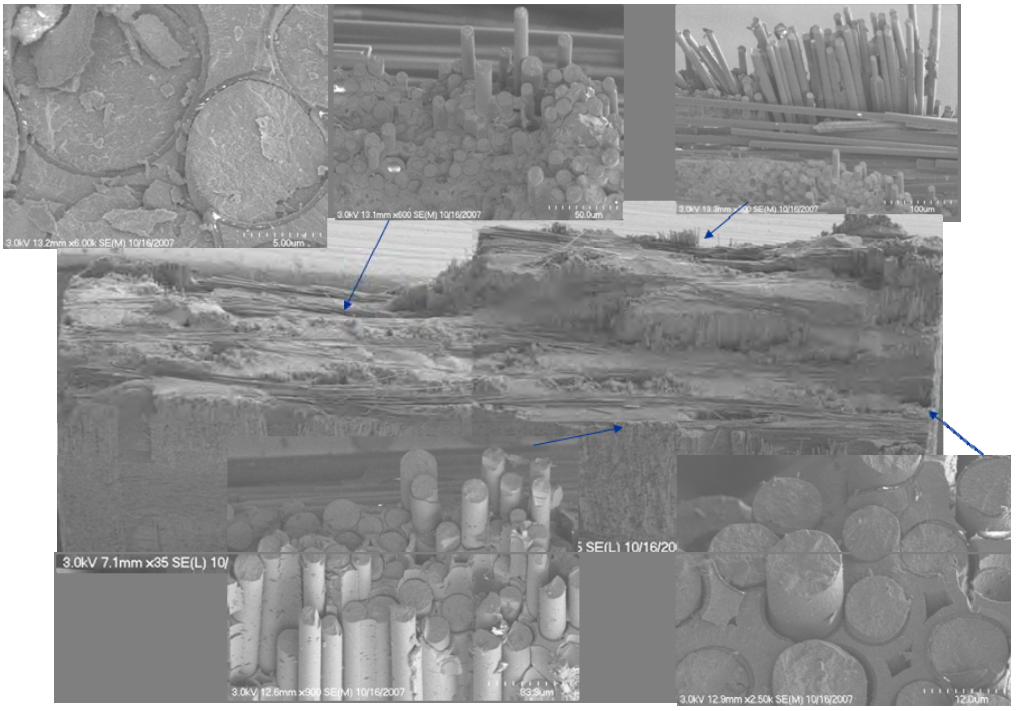

(b)

Figure 5: FESEM of a specimen subjected to (a) 220 MPa Creep followed by RT tensile to failure and (b) creep rupture at 248 MPa.

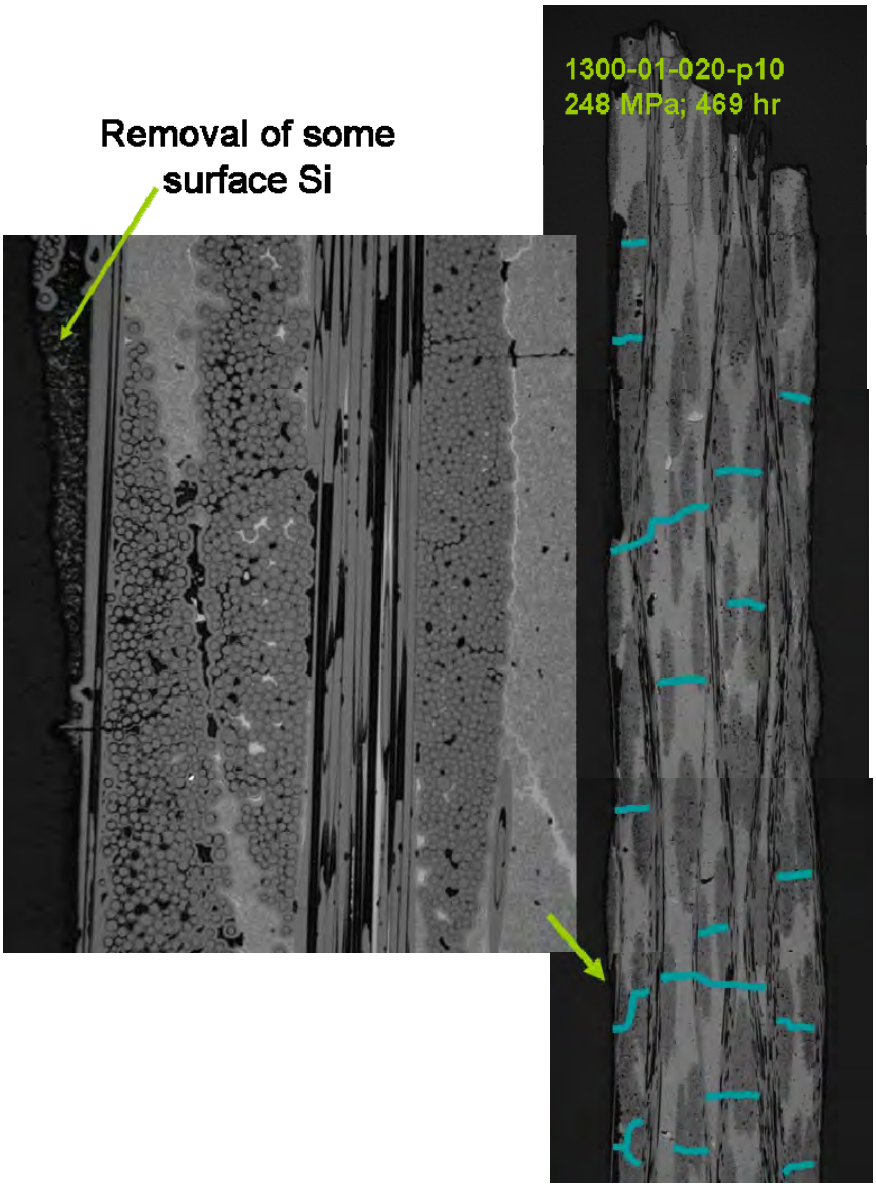

Figure 6: Optical micrographs of polished longitudinal section (blue lines in lower magnification figure highlight matrix cracks) for a 36 ksi tested specimen in vacuum.

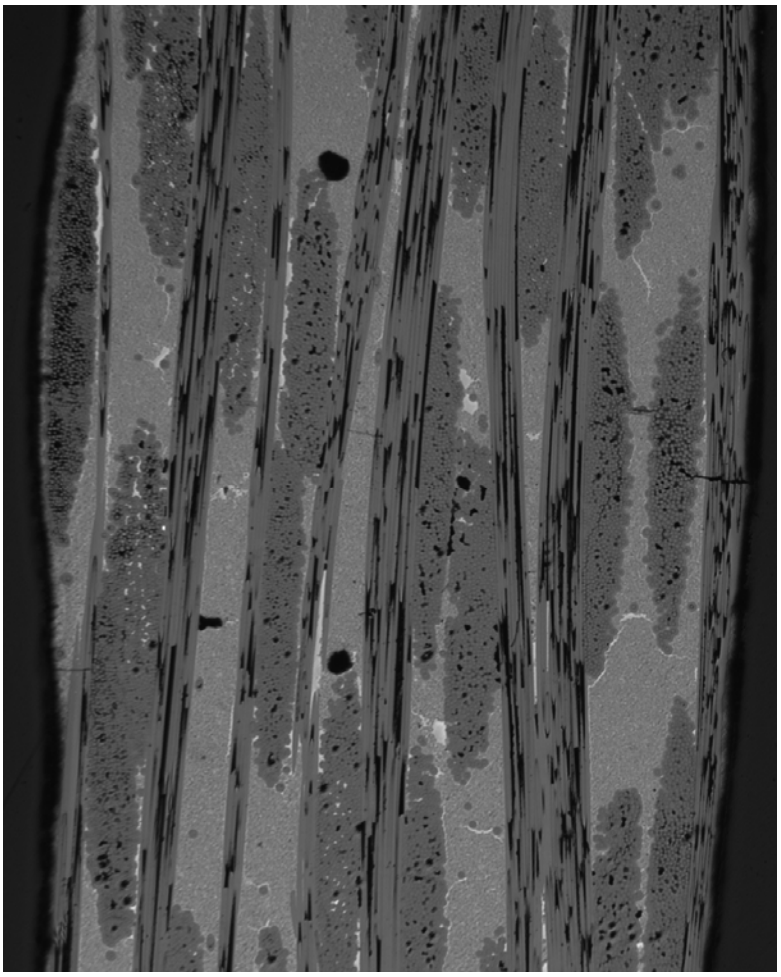

Figure 7: Polished longitudinal section showing an unbridged crack on the right side through an outer tow minicomposite for the inert tested creep rupture specimen at 220 MPa.

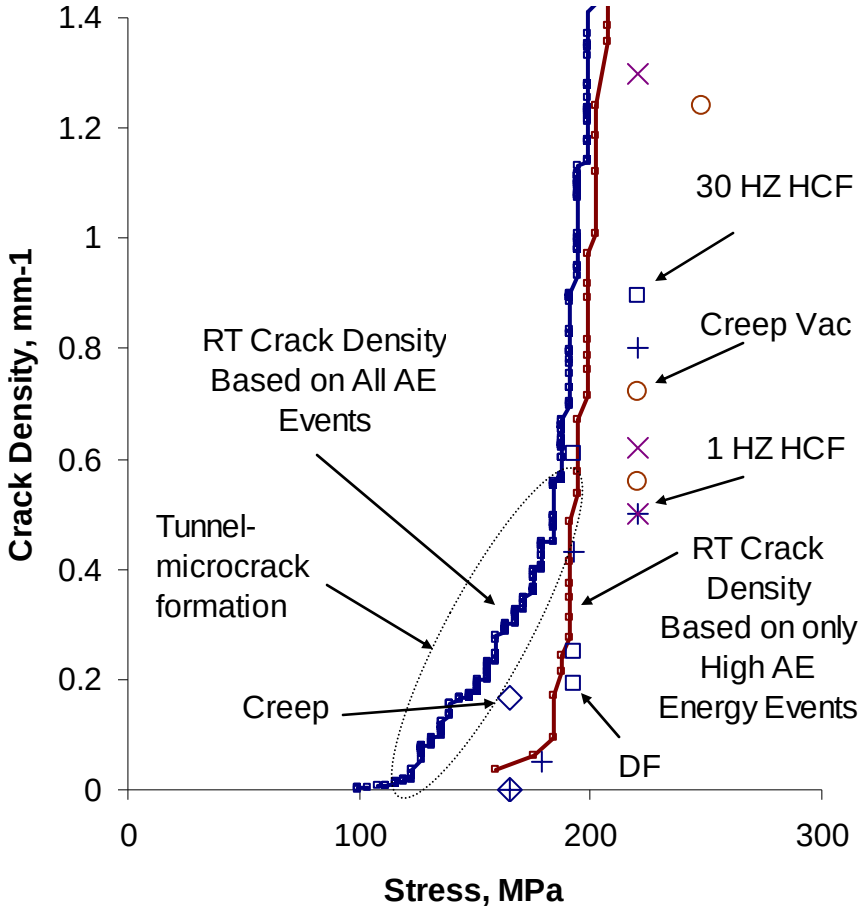

Figure 8: Matrix crack density measured along the length and compare to that estimated from room temperature acoustic emission activity (from [3]). Note that except for the highest stresses, matrix cracks were not through-thickness. The vacuum tested specimens are noted with "Vac". All other data points refer to air tested specimens [3].

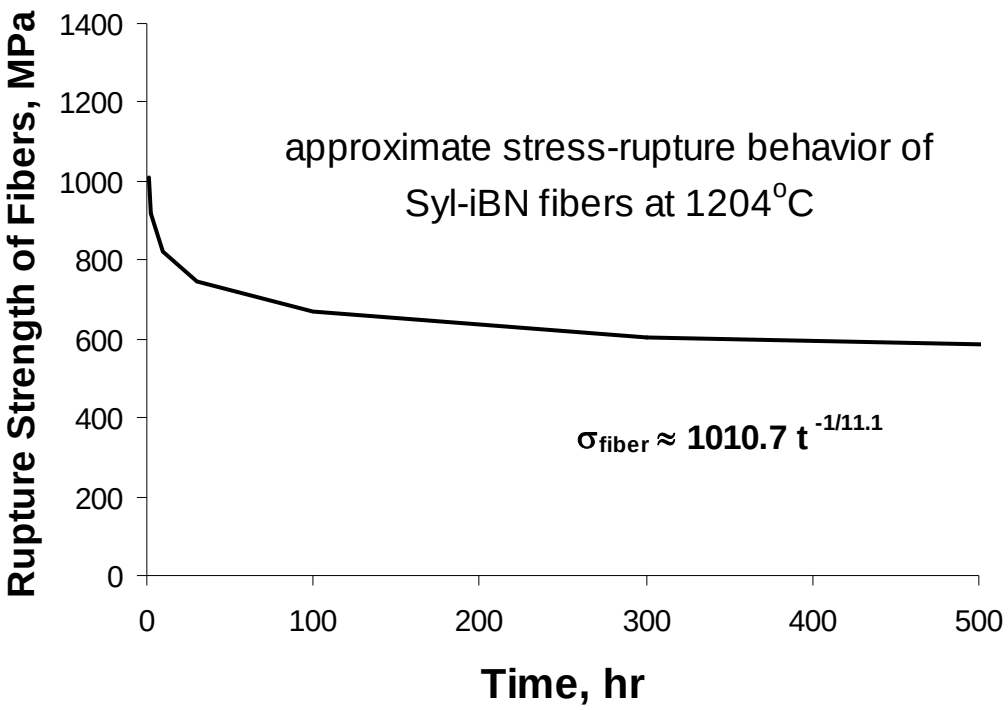

Figure 9: Stress rupture data at 1204°C for Sylramic-iBN fibers. The data was taken from a Larson-Miller plot [15].

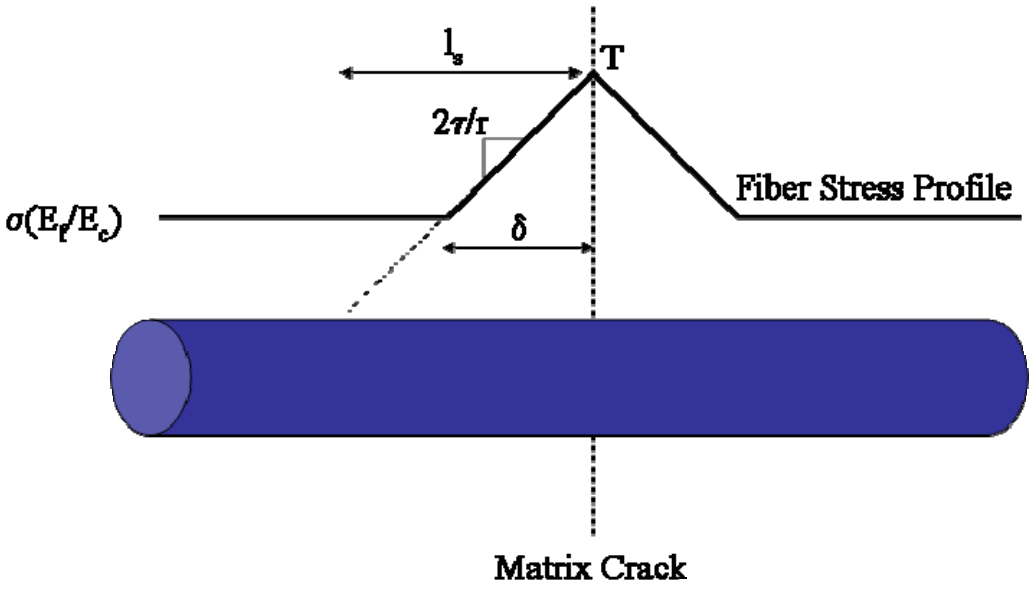

Figure 10: Stress profile of a single fiber bridging a through-thickness matrix crack (after Figure 5 in reference 17).

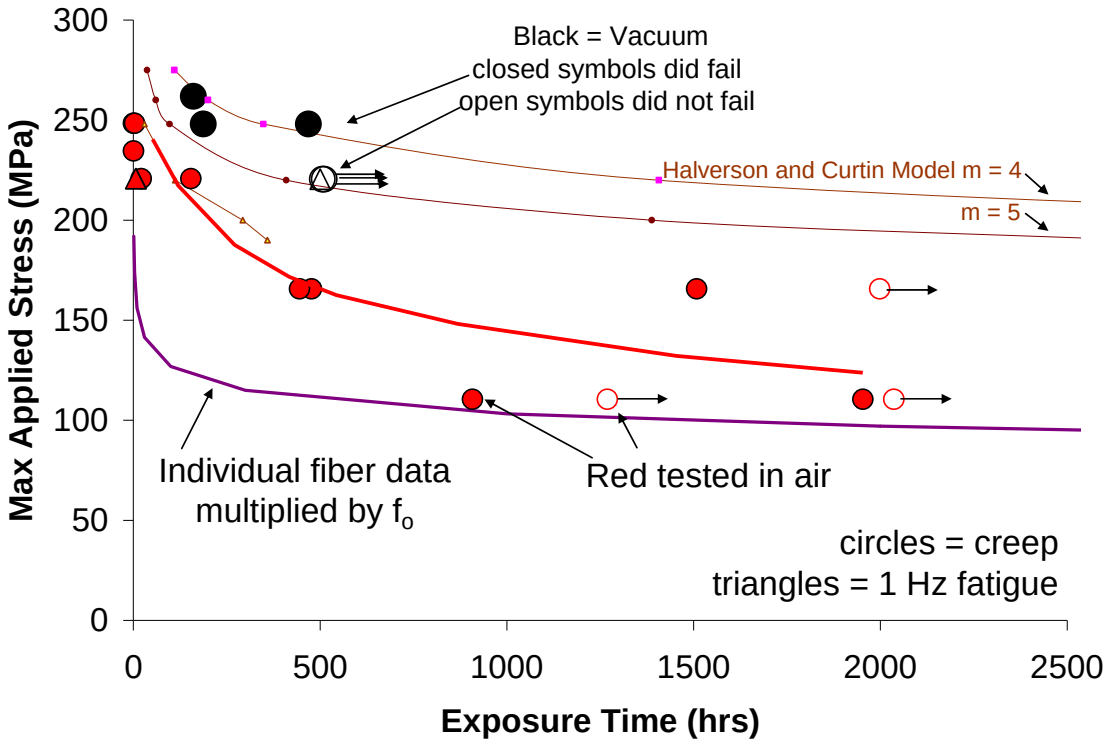

Figure 11: Creep rupture data of vacuum-tested and air-tested composites with proportioned single fiber creep rupture data [16] and the Halverson-Curtin model [17] applied to this composite system.